Giovanni News

Giovanni Image Hall of Fame 2nd Class Issue!

Editor's Note

The votes are counted; the choices have been reviewed; and the certificates are ready to be e-mailed to the authors of papers featuring an image that has been selected to enter the Giovanni Image Hall of Fame.

As this is the second time that images have been selected for the Giovanni Image Hall of Fame, these images are in the *2nd Class*. That does not mean they are any less deserving than the Inaugural Class; in fact, most of these images are related to recent events and observations. A broad variety of topics is represented in the 2nd Class, with several images related to remarkable observations and noteworthy geophysical events.

So I won't keep you any longer. Read on to see what images were selected (and why they were selected) to the 2nd Class of the Giovanni Image Hall of Fame!
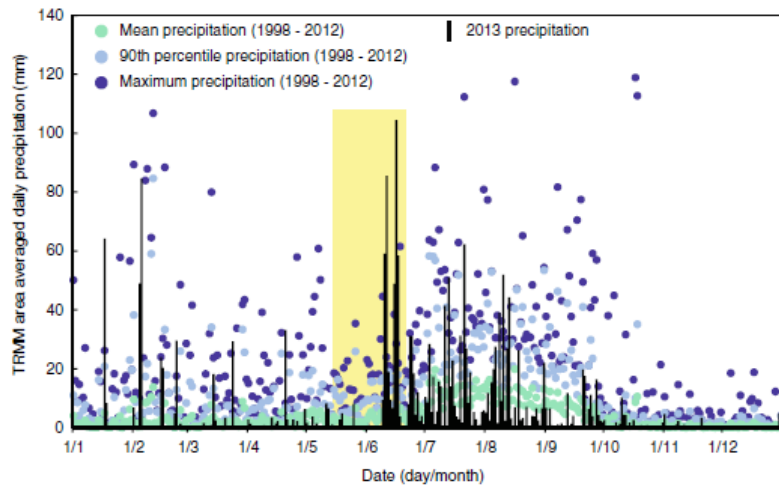
Jim Acker
The Giovanni News Editor

Fig. 4 TRMM area averaged daily precipitation over Kedarnath. Daily measurements during 2013 are compared to the longer term (1998–2012) mean, maximum and 90th percentile values. The 4-week period preceding and including the June 16–17 debris flow/lake outburst disaster is highlighted (*yellow shading*)
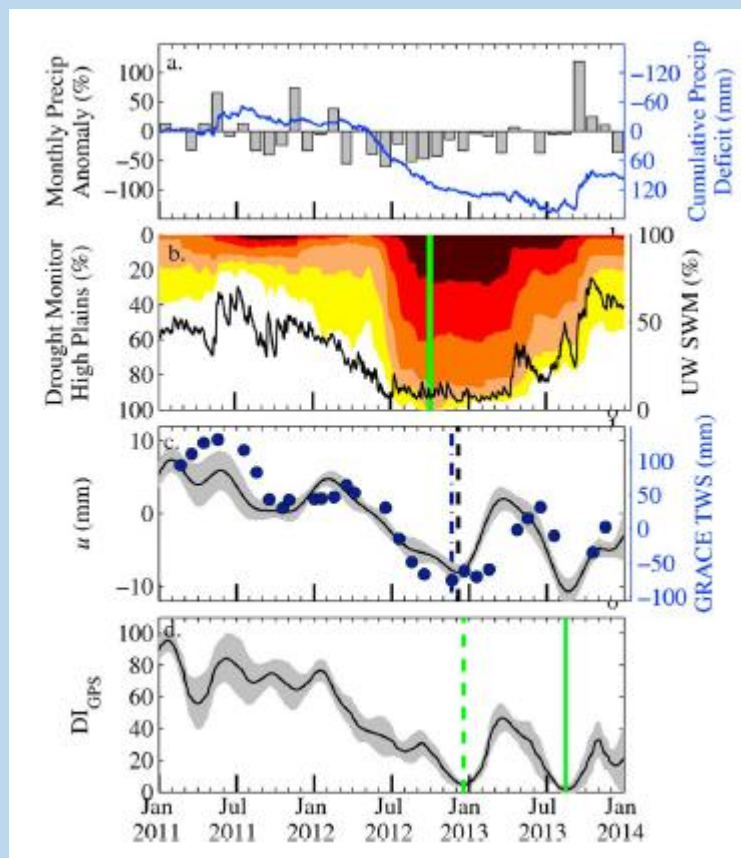
- *For Figure 4 in the paper*

Allen, S.K., Rastner, P., Arora, M., Huggel, C., and Stoffel, M. (2015) Lake outburst and debris flow disaster at Kedarnath, June 2013: hydrometeorological triggering and topographic predisposition. *Landslides*, 19 May 2015.

- This image is selected for outstanding use and depiction of Tropical Rainfall Measuring Mission (TRMM) precipitation data, and for clearly demonstrating its association with a significant geophysical Event and human tragedy, the Kedarnath landslide disaster.

- *For Figure 3 in the paper*

Chew, C.C., and Small, E.E. (2014) Terrestrial water storage response to the 2012 drought estimated from GPS vertical position anomalies. *Geophysical Research Letters*, 4 September 2014.

- This image is selected as an outstanding example of a multiple time-series figure, incorporating North American Land Data Assimilation System (NLDAS) precipitation data, along with United States Drought Monitor (USDM) and University of Washington Surface Water Monitor (SWM) indices; Global Positioning System (GPS) vertical position data; GRACE terrestrial water storage data; and DI_{GPS}, a metric of drought intensity.   The subject of the study was the 2012 drought in the U.S. Midwest.
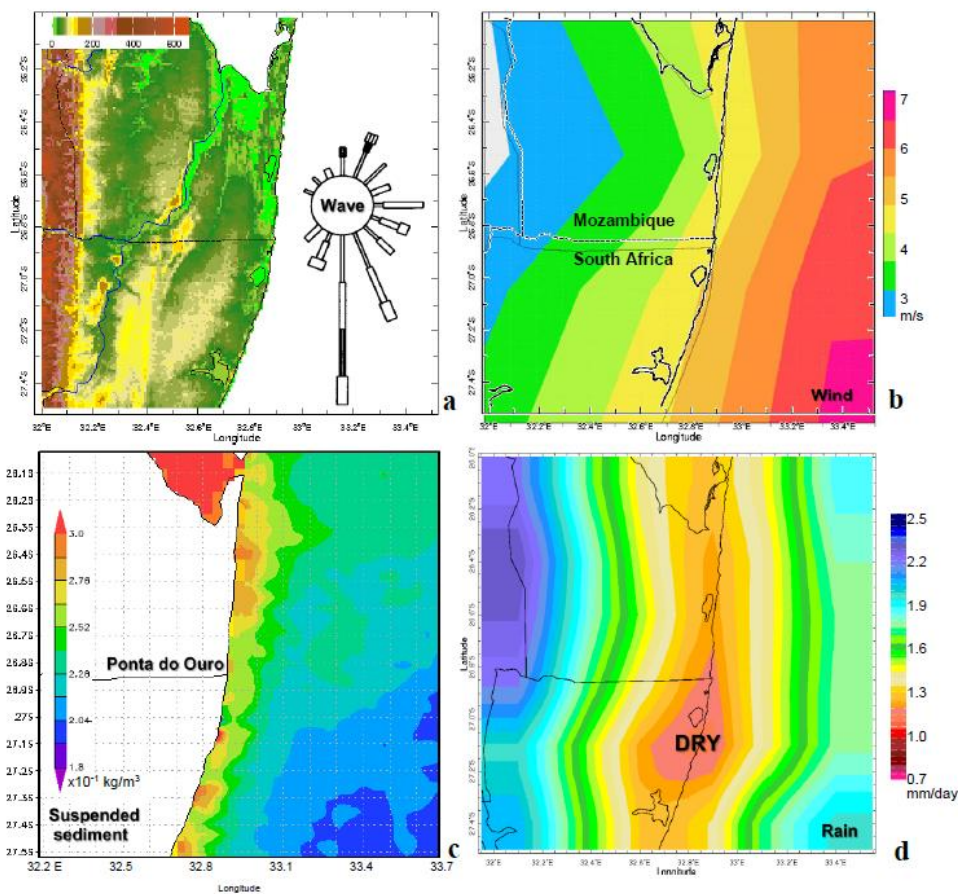
Figure 1. (a) Topography. 2000-2013 averages of (b) CFS wind speed, (c) NASA satellite suspended sediment, (d) cMorph satellite rainfall. Inset in (a) is ocean wave direction (from) and height rose at 5% (length) and 1 m (thickness) intervals. Refer to Figure 6 for large-scale context.

- *For Figure 1 in the paper*

Jury, M.R. (2015) Coastal climate and beach dynamics at Ponta do Ouro, Mozambique. *Scientific Research and Essays*, **10(1)**, 1-13.

- This image is selected for combining land surface topography, ocean wave direction and height, wind speed, suspended sediment concentrations, and rainfall data in a colorful depiction of the factors affecting coastal variability for the beach located at Ponta do Ouro, Mozambique. Suspended sediment concentrations were derived from NASA satellite data, and euphotic depth data were also utilized in the study.
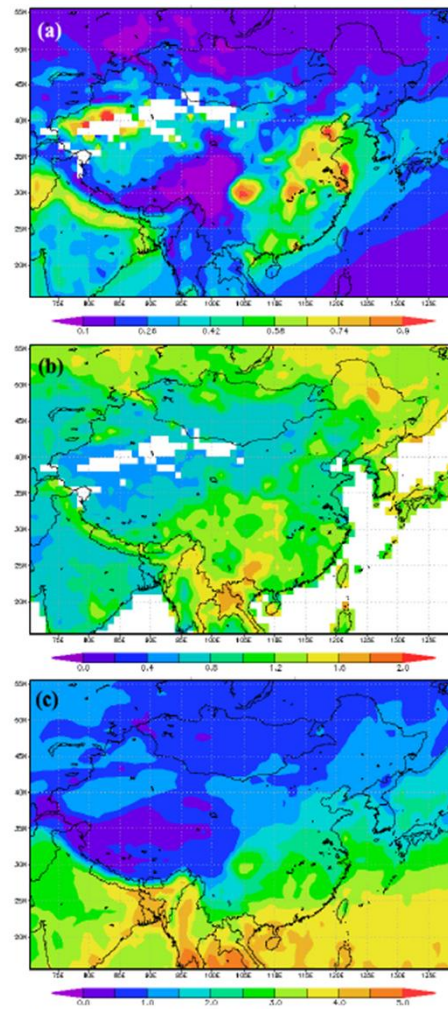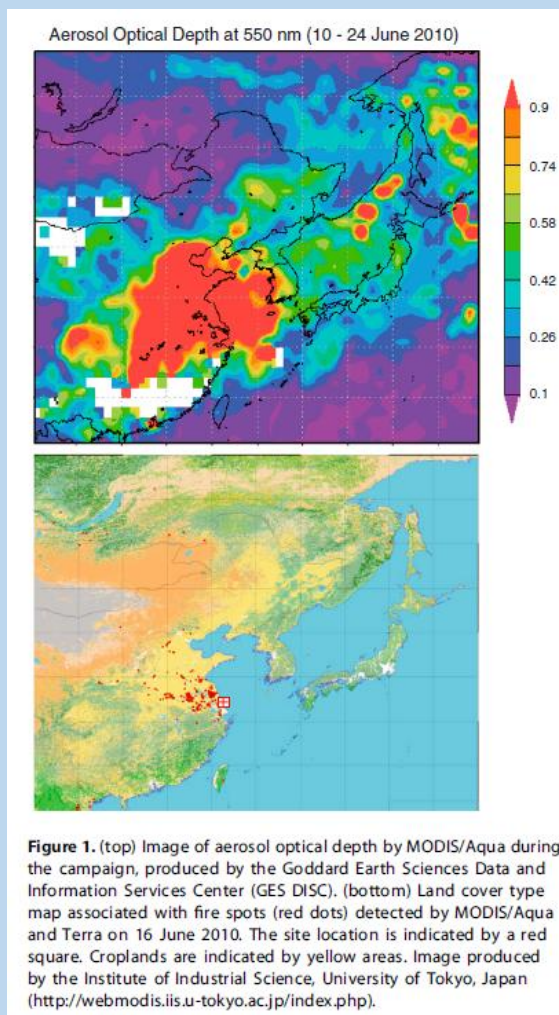
Fig. 2. Spatial distribution of ten-year averaged (a) AOD_{550} (b) Ångström exponent (AE, $\alpha_{470/660}$) and (c) Water vapor (WV) over China retrieved from MODIS Terra products for the period 2003–2013. The locations of 12 study regions are the same as that shown in Fig. 1.

- *For Figure 2 in the paper*

Kang, N., Kumar, R., Yin, Y., Diao, Y., and Yu, X. (2014) Correlation analysis between AOD and cloud parameters to study their relationship over China using MODIS data (2003–2013): impact on cloud formation and climate change. *Aerosol and Air Quality Research*, **15**, 958–973.

- This three-panel figure is selected for combining three images created with Giovanni of Moderate Resolution Imaging Spectroradiometer (MODIS) aerosol optical depth, Ångström exponent, and water vapor data over China, for the period 2003-2013.

Figure 1. (top) Image of aerosol optical depth by MODIS/Aqua during the campaign, produced by the Goddard Earth Sciences Data and Information Services Center (GES DISC). (bottom) Land cover type map associated with fire spots (red dots) detected by MODIS/Aqua and Terra on 16 June 2010. The site location is indicated by a red square. Croplands are indicated by yellow areas. Image produced by the Institute of Industrial Science, University of Tokyo, Japan (http://webmodis.iis.u-tokyo.ac.jp/index.php).

- *For Figure 1 in the paper*

Kudo, S., Tanimoto, H., Inomata, S., Saito, S., Pan, X., Kanaya, Y., Taketani, F., Wang, Z., Chen, H., Dong, H., Zhang, M., and Yamaji, K. (2014) Emissions of nonmethane volatile organic compounds from open crop residue burning in the Yangtze River Delta region, China. *Journal of Geophysical Research: Atmospheres*, **119 (12),** 7684-7698.

- The two-panel figure in Kudo *et al.* is selected for providing an easy-to comprehend depiction of the association between biomass fire locations, land cover type, and Moderate Resolution Imaging Spectroradiometer (MODIS) aerosol optical depth (AOD) data. The MODIS AOD data were averaged over the period of the observational campaign, June 10-24, 2010.
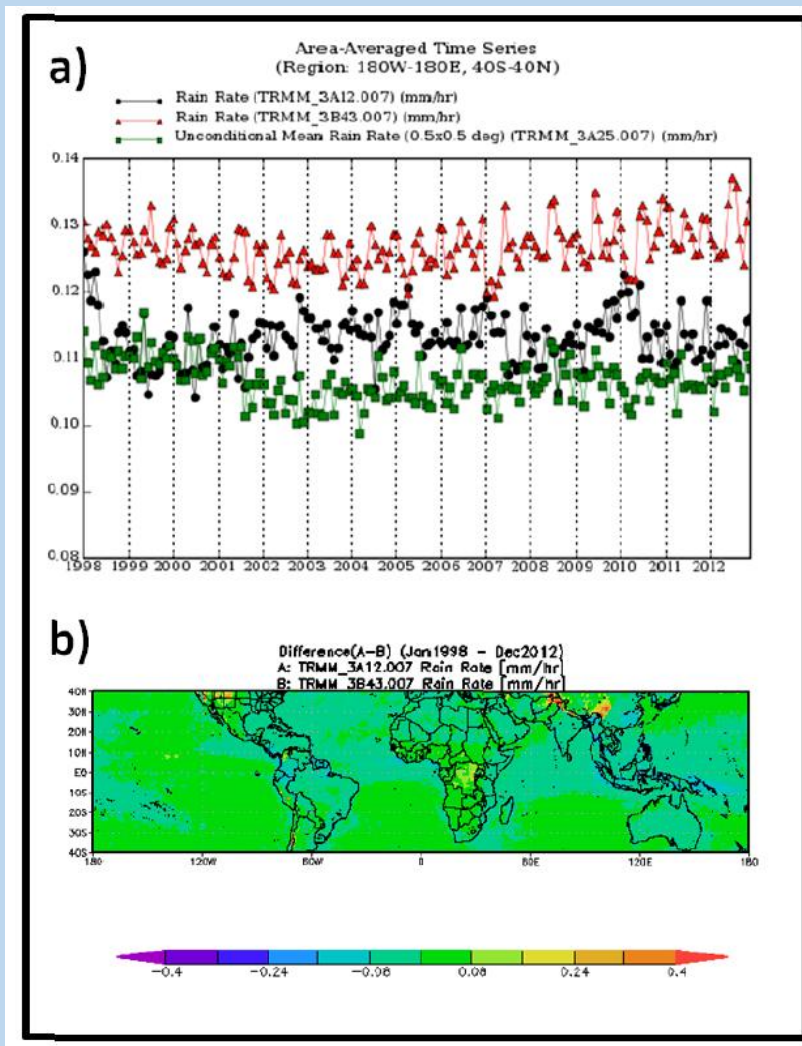
- *For Figure 6 in the paper*

Liu, Z., Ostrenga, D., Teng, W., Kempler, S., and Milich, L. (2014) Developing GIOVANNI-based online prototypes to intercompare TRMM-related global gridded-precipitation products. *Computers & Geosciences*, 66, 168-181.

- This image is selected for demonstrating an important application of the use of Giovanni, data intercomparison – in this case a spatial and time-series intercomparison of rain rate data from the TRMM_3A12.007, TRMM_3B43.007, and the TRMM_3A25.007 data products.
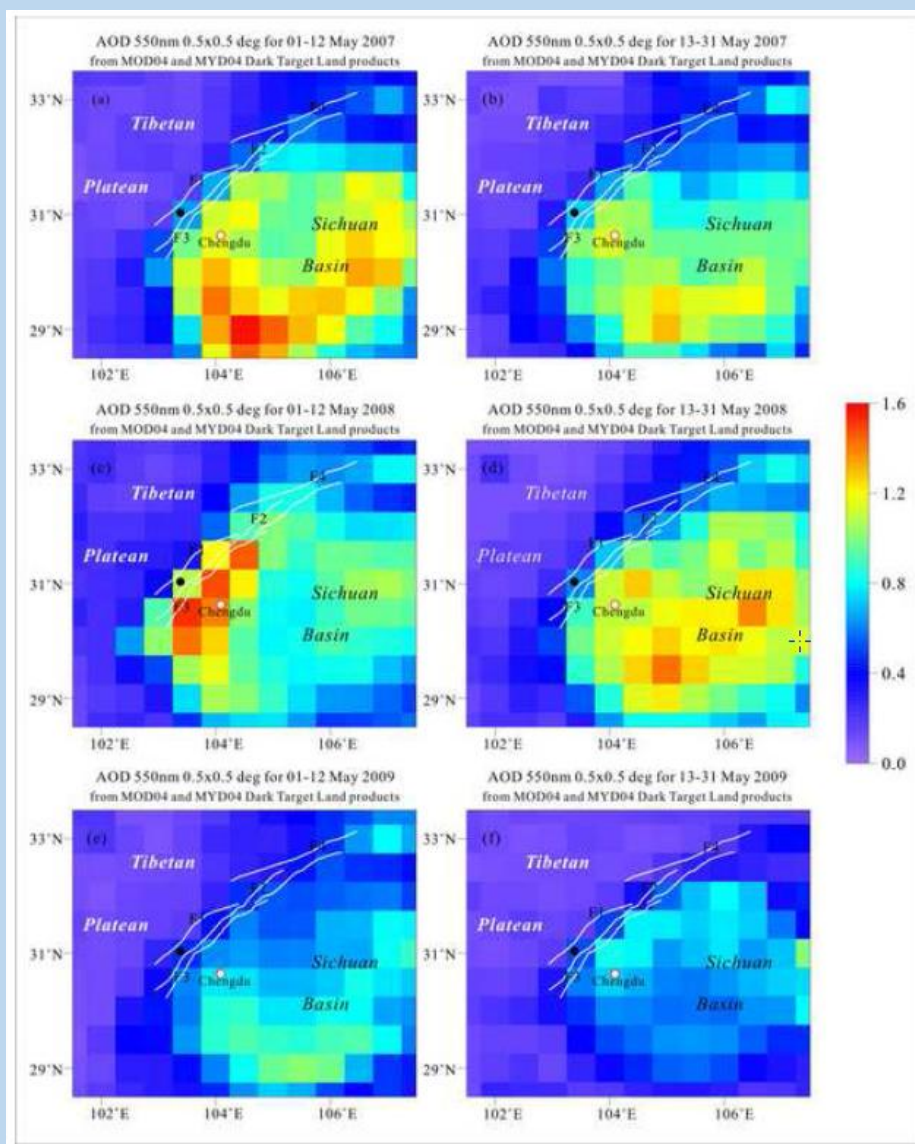
- *For Figure 1 in the paper*

Qin, K., Wu, L.X., Zheng, S., Bai, Y., Lv, X. (2014) Is there an abnormal enhancement of atmospheric aerosol before the 2008 Wenchuan earthquake? *Advances in Space Research,* **54(6),** 1029-1034.

- These images are selected for using Giovanni to depict the remarkable increase in observed atmospheric aerosol optical depth along the Longmenshan faults preceding the 2008 Wenchuan (China) earthquake. This constitutes one of the most intriguing observations made with data available in Giovanni appearing in published research.
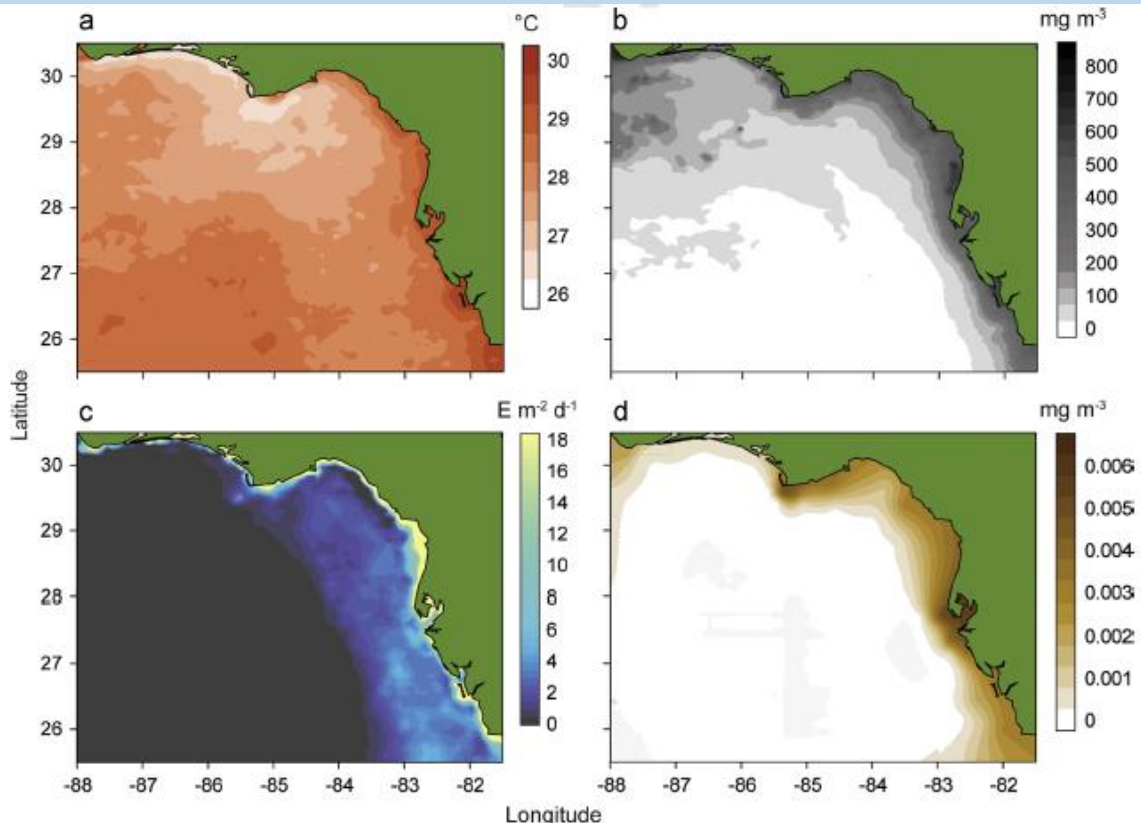
Fig. 3. Sea surface temperature (a), particulate organic carbon concentration (b), photosynthetically active radiation at the bottom of the West Florida Shelf (c), and particulate inorganic carbon concentration (d) in the summer of 2009. (a) Sea surface temperature (SST), (b) Particulate organic carbon (POC), (c) Light at depth (PAR(z)) and (d) Particulate inorganic carbon (PIC).

- *For Figure 3 in the paper*

Radabaugh, K.R., and Peebles,E.B. (2014) Multiple regression models of δ^{13}C and δ^{15}N for fish populations in the eastern Gulf of Mexico. *Continental Shelf Research*, **84**, 158-168.

- This four-panel figure is selected for demonstrating a useful "recoloration" of ocean color data acquired by Giovanni (sea surface temperature, particulate organic carbon, photosynthetically available radiation, and particulate inorganic carbon) for background information in the study.
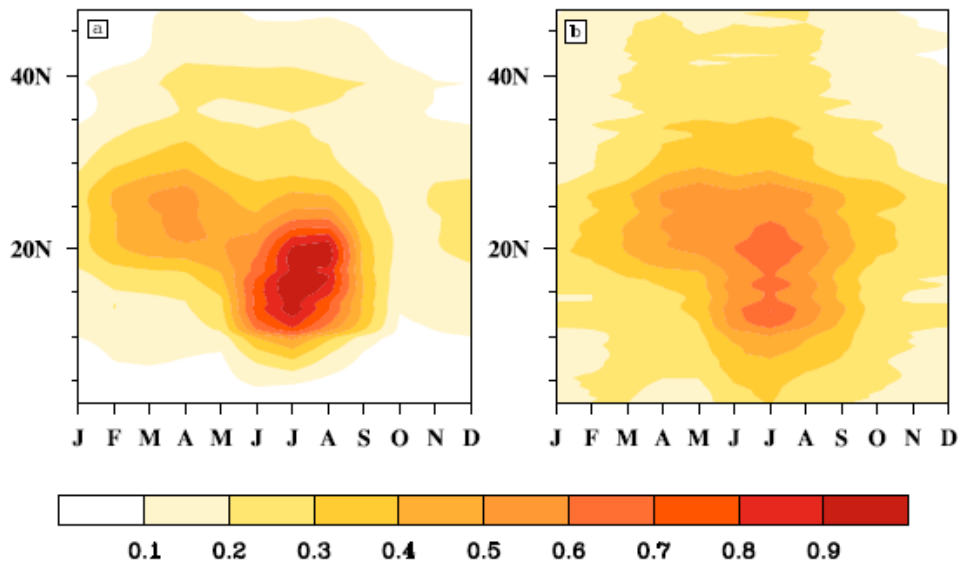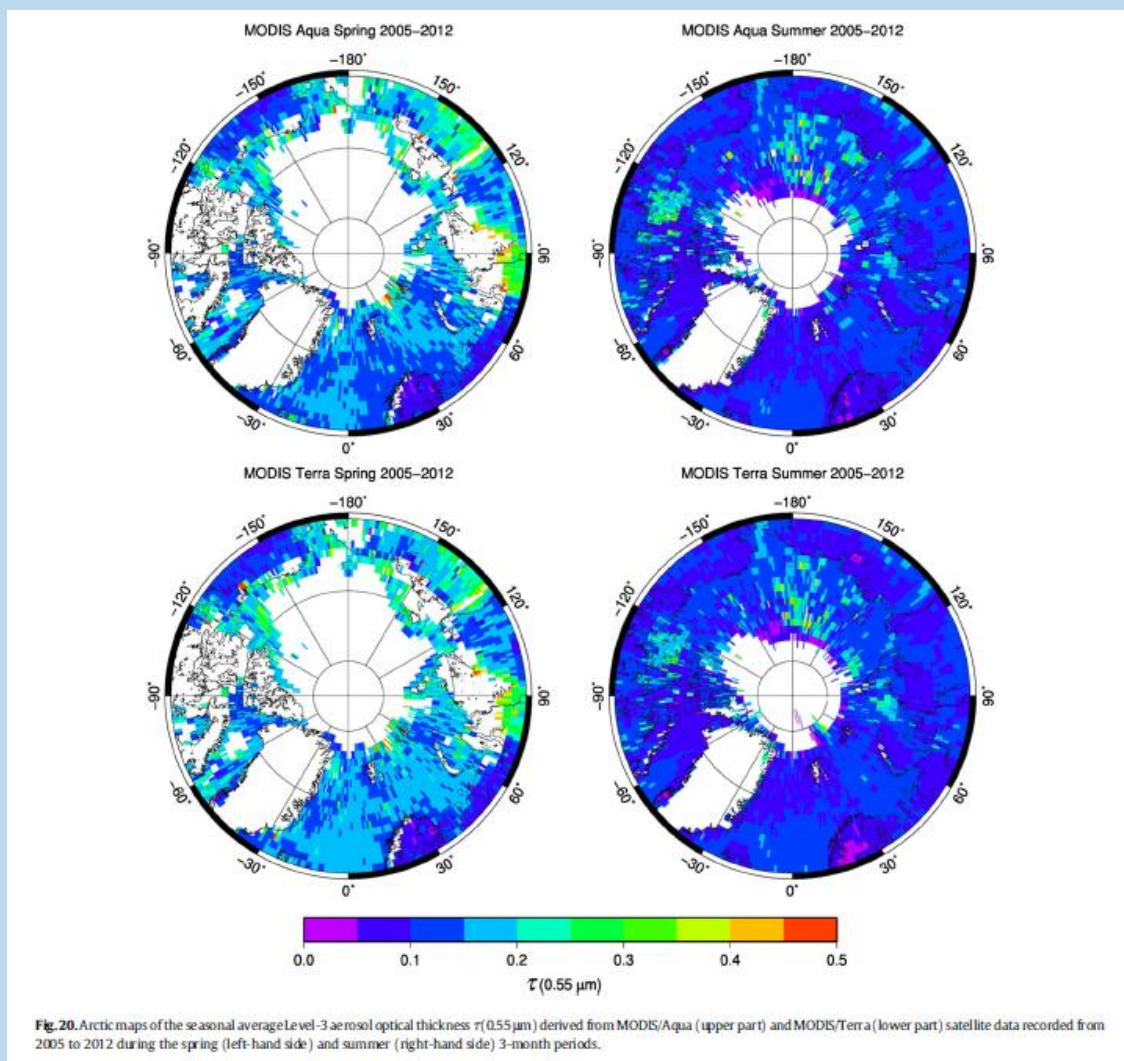
Figure 3. The annual cycle of the zonally averaged AOD (averaged from 44 to 56° E and over the 13 year simulation period), **(a)** RegCM4.4 AOD, **(b)** MISR AOD.

- *For Figure 3 in the paper*

  Shalaby, A., Rappenglueck, B., and Eltahir, E.A.B. (2015) The climatology of dust aerosol over the Arabian peninsula. *Atmospheric Chemistry and Physics Discussions*, **15**, 1523–1571.

- This figure is selected for the simple depiction of a comparison of an annual cycle between RegCM4.4 model output and a Hovmöller diagram generated by Giovanni of Multi-angle Imaging Spectroradiometer (MISR) data.

MODIS Aqua Spring 2005–2012

MODIS Aqua Summer 2005–2012

MODIS Terra Spring 2005–2012

MODIS Terra Summer 2005–2012

τ (0.55 μm)

Fig. 20. Arctic maps of the seasonal average Level-3 aerosol optical thickness τ (0.55 μm) derived from MODIS/Aqua (upper part) and MODIS/Terra (lower part) satellite data recorded from 2005 to 2012 during the spring (left-hand side) and summer (right-hand side) 3-month periods.

- *For Figure 20 in the paper*

Tomasi, C., Kokhanovsky, A.A., Lupi, A., Ritter, C., Smirnov, A., O'Neill, N.T., Stone, R.S., Holben, B.N., Nyeki, S., Wehrli, C., Stohl, A., Mazzola, M., Lanconelli, C., Vitale, V., Stebel, K., Aaltonen, V., de Leeuw, G., Rodriguez,, E., Herber, A.B., Radionov, V.F., Zielinski, T., Petelski, T., Sakerin, S.M., Kabanov, D.M., Xue, Y., Mei, L., Istomina, L., Wagener, R., McArthur, B., Sobolewski, P.S., Kivi, R., Courcoux, Y., Larouche, P., Broccardo, S., and Piketh, S.J. (2014) Aerosol remote sensing in polar regions. *Earth-Science Reviews*, **140**, 108–157.

- The image from Tomasi *et al*. is selected for using Giovanni to create polar projections of Arctic maps of the seasonal average Level-3 Moderate Resolution Imaging Spectroradiometer (MODIS) aerosol optical thickness τ (0.55 μm) for the period 2005-2012.
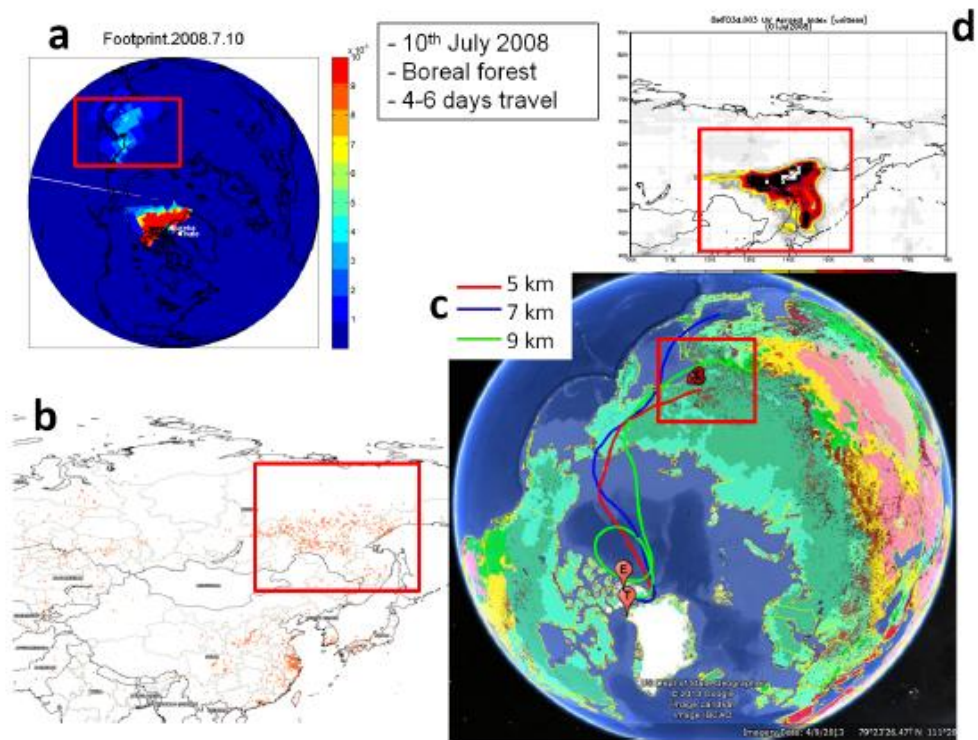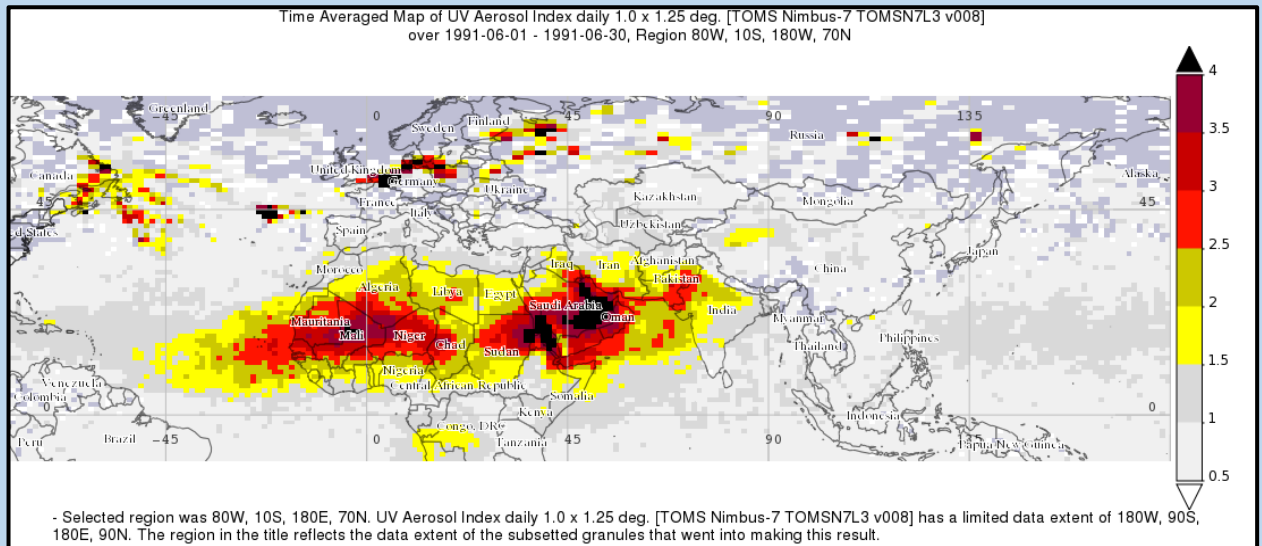
Figure 4. Example of attribution of fire source region and transport time for the event number 3, detected at Eureka on the 10 July 2008. **(a)** STILT footprints for that day, **(b)** MODIS fire hot spots, **(c)** HYSPLIT backtrajectories ending that day, **(d)** OMI UV aerosol index for that day.

- *For Figure 4 in the paper*

Viatte, C., Strong, K., Hannigan, J., Nussbaumer, E., Emmons, L., Conway, S., Paton-Walsh, C., Hartley, J., Benmergui, J., and Lin, J. (2014) Identifying fire plumes in the Arctic with tropospheric FTIR measurements and transport models. *Atmospheric Chemistry and Physics*, **15**, 2227-2246.

- This figure was selected for its amalgamation of images providing a comprehensive and visually satisfying summary of the paper's subject. Moderate Resolution Imaging Spectroradiometer (MODIS) fire hot spots and Ozone Measuring Instrument UV aerosol data depicted with Giovanni are combined with particulate transport models and air mass trajectories in this figure.

Time Averaged Map of UV Aerosol Index daily 1.0 x 1.25 deg. [TOMS Nimbus-7 TOMSN7L3 v008] over 1991-06-01 - 1991-06-30, Region 80W, 10S, 180W, 70N

- Selected region was 80W, 10S, 180E, 70N. UV Aerosol Index daily 1.0 x 1.25 deg. [TOMS Nimbus-7 TOMSN7L3 v008] has a limited data extent of 180W, 90S, 180E, 90N. The region in the title reflects the data extent of the subsetted granules that went into making this result.

- K. Potts, for the image entitled *Giovanni 4 image of the TOMS aerosol index from the Nimbus 7 satellite for June 1991*.

  - This image is selected for its use of Giovanni-4 to depict three different aerosol plumes: smoke from oil field fires in Kuwait set after the end of the war; dust from the Bodélé depression in Chad; and sulfur aerosol from the volcanic eruption of Mount Pinatubo in the Philippines. This user-generated image includes effects from geopolitical affairs, climate change, and a significant geophysical event. The submitter is the only individual or group to have an image selected to both the Inaugural Class and 2nd Class of the Giovanni Image Hall of Fame.